

Original Investigation

Computer-aided Diagnosis via Model-based Shape Analysis: Automated Classification of Wall Motion Abnormalities in Echocardiograms¹

Johan G. Bosch, MSc, Francisca Nijland, MD, PhD, Steven C. Mitchell, PhD, Boudewijn P.F. Lelieveldt, PhD,
Otto Kamp, MD, PhD, Johan H.C. Reiber, PhD, Milan Sonka, PhD

Rationale and Objective. Shape analysis of endocardial contour sequences from echocardiograms can provide classification of wall motion abnormalities (WMA).

Materials and Methods. We previously reported on active appearance motion models (AAMM) for automated detection of endocardial contours in sequences of echocardiograms. The shape analysis of AAMM renders eigenvariations of shape/motion, including typical normal and pathologic endocardial contraction patterns. A set of stress echocardiograms (single-beat four-chamber and two-chamber sequences with expert-verified endocardial contours) of 129 infarct patients was split randomly into training ($n = 65$) and testing ($n = 64$) sets. AAMMs were generated from the training set and AAMM shape coefficients (ASCs) were extracted for all sequences and statistically related to regional/global visual wall motion scoring (VWMS) and volumetric parameters.

Results. Linear regression showed clear correlations between ASCs and VWMS. Discriminant analysis showed good prediction by ASCs of both segmental (74% correctness) and global WMA (90% correctness). Volumetric parameters correlated poorly to regional VWMS.

Conclusion. 1) ASCs show promising accuracy for automated WMA classification. 2) VWMS and endocardial border motion are closely related; with accurate automated border detection, automated WMA classification should be feasible. 3) ASC shape analysis allows contour set evaluation by direct comparison to clinical parameters.

Key Words. Computer aided diagnosis; principal component analysis; shape sequence analysis; active appearance models; cardiac ultrasound.

© AUR, 2005

The visual detection of wall motion abnormalities (WMA) in echocardiograms is an important diagnostic issue. Detecting such WMA (abnormal contraction patterns of the myocardium of the left ventricle) forms the basis of stress echocardiography (1), a widely applied diagnostic technique. Stress echo is now solely evaluated visually and although the technique is well validated, it is known to be subject to high inter- and intraobserver variability and high interinstitution variability (2). For the physician, it also requires a long training process and is cumbersome to perform. Therefore, both the applicability and the reli-

Acad Radiol 2005; 12:358–367

¹ From Leiden University Medical Center, Leiden, The Netherlands (J.G.B., B.P.F.L., J.H.C.R.); The University of Iowa, Iowa City, Iowa (S.C.M., M.S.); Vrije Universiteit Medical Center, Amsterdam, The Netherlands (F.N., O.K.). Received March 29, 2004; revision received November 1; revision accepted November 17. Supported in part by the Ministry of Economic Affairs, The Netherlands (BTS00123), and by the National Institutes of Health (R01 HL071809). **Address correspondence to:** M.S. e-mail: milan-sonka@uiowa.edu

© AUR, 2005

doi:10.1016/j.acra.2004.11.025

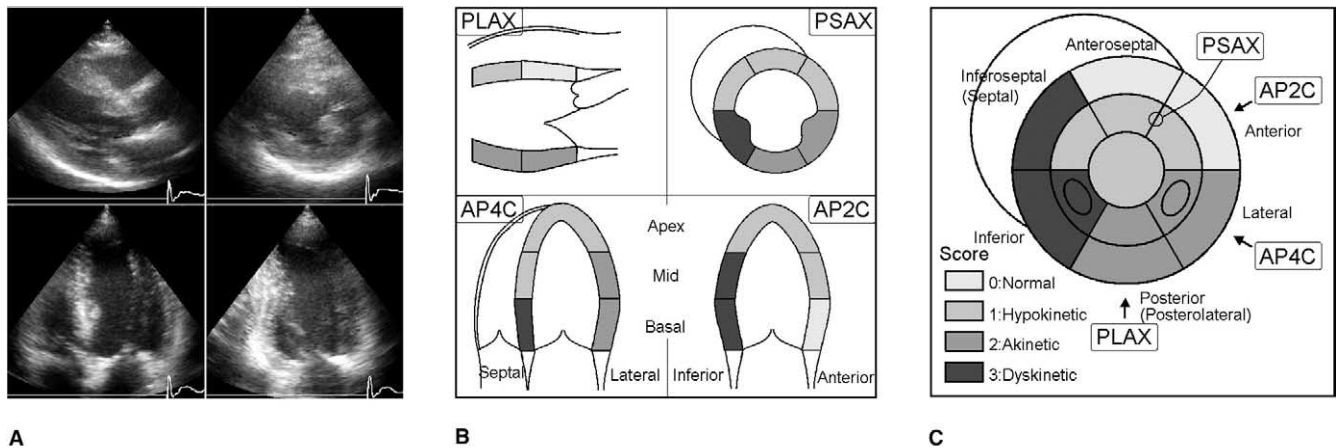


Figure 1. Stress echocardiogram in practice. (a) Quad-screen of synchronized views. (b) Schematic views with scored segments. (c) Bull's eye representation (13 segments, four scoring levels as employed in this study).

ability of stress echo could benefit from automated analysis and automated classification of WMA. The purpose of this study was to evaluate a new approach to such an automated classification.

MATERIALS AND METHODS

Stress Echo and Visual Wall Motion Scoring

Stress Echo is a diagnostic technique for noninvasive assessment of left ventricular (LV) dysfunction and suspected coronary artery disease by studying the LV regional wall motion patterns in echocardiographic images. Comparing these patterns when the patient is at rest with a state of stress (maximum workload for the myocardial muscle, invoked either by physical exercise or by a pharmacologic agent such as dobutamine) allows the detection of several types of myocardial tissue conditions, such as ischemia, necrosis (infarct), and hibernation. Deteriorating contractility in one or more segments in stress is a sign of local ischemia and is associated with a stenosis in the corresponding coronary artery. For stress echo, images are acquired in standard cross sections or views (generally apical four-chamber, apical two-chamber, parasternal long axis, and parasternal short axis). These views are acquired at rest and under several levels of stress. Typically, one complete heart beat per view is selected. These beats are synchronized and replayed as a loop in a quad screen (Fig. 1A). Wall motion for the different segments of the LV wall is assessed visually. A qualitative score (such as normal or hypokinetic) is assigned

to each segment; this process is named visual wall motion scoring (VWMS). Different scoring systems are in use; the data we describe in this study use a 4-point scoring system (0: normokinesia; 1: hypokinesia; 2: akinesia; 3: dyskinesia) and 13 segments (Fig. 1B,C). The scoring is generally presented graphically (Fig. 1B) by coloring the segments in a schematic drawing of the four views or in a so-called bull's eye plot (Fig. 1C, a projection map of the whole LV wall as seen from the apex). Each scoring level is associated with a numeric value so that semiquantitative results can be calculated, such as the total score of all segments, the score index (average score for the number of available segments), and similar numbers for the groups of segments associated with one of the coronary arteries. Although differences in scores between rest and stress play an important role, the absolute scores have diagnostic value as well. Therefore, development of an automatic method for classification of wall motion similar to the visual wall motion scores is highly desirable. We expect that (automatic) detection of the endocardial borders and subsequent analysis of the found endocardial shapes gives the best chance of achieving automated classification.

Analysis of Endocardial Shapes

Provided that endocardial contours have been outlined accurately (either manually or automatically), deriving a measure for regional wall motion from such contours is not straightforward. Many parameters of size, shape, and displacement have been suggested for wall motion analy-

sis—regional contribution to ejection fraction and regional displacements with and without global motion correction (3), systolic change of log LV volume (4), peak systolic velocity (5), segmental radial and longitudinal velocity (6)—but relation to wall motion scores was mostly of medium to weak strength. Partly this may be attributed to the inherent variabilities in VWMS itself, partly to the limitations of the applied measures (eg, either too global or too local; sensitivity to disturbing factors such as overall heart motion, minor temporal or spatial mispositioning). Furthermore, we presume that more is involved in VWMS than estimating absolute local displacement, such as wall thickening, endocardial shape itself, and specific local and global motion patterns over the full cardiac cycle. Therefore we expect that more descriptive and subtle parameters of shape are required to allow assessment of WMA.

During our developments of automated border detection methods, we noticed that the shape modeling approach employed in the so-called active appearance Model (AAM) approach (as described in the following section) might be useful for shape classification purposes. This shape modeling is based on principal component analysis (PCA), a statistical technique that models the variability within a large set of examples. In terms of shapes, PCA finds the average endocardial shape and the main modes of variation (so-called eigenvariations or eigenvectors of shape/motion) over a group of patients. Thus PCA captures typical motion patterns associated with cardiac contraction. Any shape in the set can be accurately described as the average shape plus a specific linear combination of these eigenvariations. Thus all shapes can be compactly and completely described by their AAM shape coefficients (ASCs), a small set of numbers (about 60 in our case). Moreover, some eigenvariations of shape/motion seemed to correspond to typical pathologic patterns (Fig. 2). Therefore, we hypothesized that ASCs could be useful for classification of WMAs.

Automated Border Detection and Active Appearance Models

For automated detection of the desired endocardial borders in sequences of echocardiograms, we have previously presented several approaches, including semi-automated techniques based on dynamic programming and pattern matching (7,8) and fully automated techniques based on AAM. AAM is a highly promising segmentation technique that was introduced by Cootes et al. and has been extensively described in many arti-

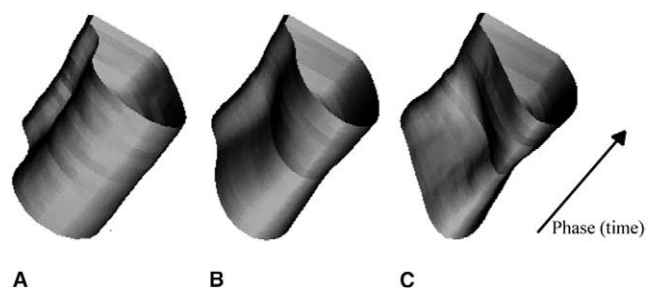


Figure 2. Second eigenvariation of endocardial shape/motion from an active appearance motion model for four-chamber sequences (mean shape (b) plus and minus (a, c) 3 standard deviations). The objects show contour sequences expressed as a single shape sample. The open ends of the “tube” represent the end-diastolic phases, whereas the constriction in the middle corresponds to end-systole. This eigenvariation is related to typical pathology: apex dilation (a) is generally associated with reduced apical contraction.

cles (9–11). An AAM completely describes both image appearance and object shape over a set of examples as a combined statistical shape-appearance model. AAMs model the complete object appearance, including typical local, position-dependent artifacts. Ultrasound images are generally acquired in standardized cross-sections, and artifacts typically occur in the same parts of the anatomy (such as lateral wall dropouts). Furthermore, because AAMs are trained from expert-segmented examples, they mimic the expert’s segmentation decisions in cases of typical artifacts. All this makes AAMs highly suitable for ultrasound segmentation. Details of our different extensions of AAM toward echocardiographic segmentation are described elsewhere (12–15). The extension to modeling and detection of time sequences of echocardiograms (12,13) (the so-called active appearance motion models or AAMMs) is most important in the context of this study. PCA on the set of training time sequences in AAMMs renders the mean and eigenvariations of shape of the complete cardiac cycle. It results in an “average heartbeat,” and its characteristic motion variations over the complete cycle, as associated to normal/abnormal cardiac contraction. An example is given in Fig. 2, where it is shown that a dilation of the apex is typically associated with a reduced displacement at end-systole (hypokinesis).

A more technical description of the shape sequence modeling approach by point distribution models as employed in AAMMs in relation to shape classification can be found elsewhere (16).

As said, the purpose of the study described here was to assess the feasibility of the automated classification of WMA from AAM shape coefficients. AAM appearance modeling and border detection play a minor role here. For magnetic resonance imaging, we have published a similar approach for computer-aided diagnosis based on AAM shape coefficients (17).

Clinical Data

Low-dose dobutamine stress echoes were acquired from 129 unselected infarct patients participating in a clinical trial (18). For all patients, VWMS was performed following the scoring system described in a previous section (13 segments, scores from 0 to 3 per segment). Scores per segment and summations (total, per view, and per combination of corresponding mid- and basal segments) were determined. From the manually defined end-diastolic (ED) and end-systolic (ES) contours as described in the next section, several global LV volume measures were calculated: biplane ED and ES volumes and ejection fraction (EF), using biplane Simpson's rule; and a sphericity index for ED and ES. This is a simple shape measure specifying the ratio of the biplane volume to that of a sphere with the same diameter as the LV's long axis; a dilated ventricle has an increased sphericity index.

Image Data and Manual Border Definition

From all patients of the set, the transthoracic apical four-chamber and two-chamber image sequences from the baseline stage (nonstress) were available for border detection. Images were digitized from videotape with different calibration factors (0.28–0.47 mm/pixel). End-diastolic and end-systolic frames were marked by the expert observer. All single-beat sequences were phase-normalized to 16 frames.

The expert observer manually outlined the contours of the endocardium in ED and ES images of all image sequences. The volumetric measures listed previously were calculated from these borders. For the remaining images, a semiautomated detection was used based on these ED/ES borders (ECHO-CMS system; MEDIS Medical Imaging Systems, Leiden, The Netherlands) (8). In all cases, the expert applied manual corrections and redetection until completely satisfied with all resulting borders. In total, less than 20% of the contours was manually defined or corrected. Although this contour set can not be considered to be a manually defined set, it is completely expert validated and therefore a valid independent standard. In total, 4,128 ultrasound frames were available with an accompanying expert-validated contour.

Model Training and Shape Analysis

The total data set was split randomly into a training set of 65 patients (TRN) and a testing set of 64 patients (TST). Each contour was modeled by 37 landmark points, of which the apex and mitral valve attachments were true anatomic landmarks; the other points were defined by regular subdivision of the manually defined contours. A full-cycle shape representation of all 16 phases thus contained 592 points.

AAMMs for two-chamber and four-chamber sequences were generated from the training set and the ASCs for all training patients were extracted. This resulted in 62 eigenvectors for the two-chamber model and 63 for the four-chamber model and equivalent numbers of ASCs. Because total size of the shape might also be related to pathology, an absolute shape size estimate (calculated from the calibration and two pose parameters) was included in the analysis as well, resulting in 63 and 64 parameters, respectively. Contour sequences of the test patients (TST) were optimally approximated by the AAMM's shape model and the corresponding ASCs and pose were extracted. Note that we did not employ AAMM automated border detection, but only its shape modeling. All analyzed contours were from the set described previously.

RESULTS

We used SPSS for Windows version 9.0 (SPSS Inc., Chicago, IL) for statistical analyses on ASCs, VWMS results, and volumetric parameters. We employed multivariate linear regression and linear discriminant analysis on different combinations of parameters.

Multivariate Linear Regression With ASCs as Independents

Multivariate linear regression was performed for the different sets of ASCs (as independents) against all VWMS results and volumetric parameters (as dependents) (Table 1). R^2 values (the square of the correlation coefficient R) were determined, representing the percentage of the variability in the dependent variable that can be explained by the independent variable(s), the ASCs.

ASCs from the AAMM model appropriate for the dependent variable's view were employed. So, for VWMS of single or combined two-chamber segments, all 62 ASCs plus the size estimate from the two-chamber model. For the combined-view results (eg, the apex, the total of all 13 segments, all volumetric parameters), entering all

Table 1
Multivariate Linear Regression: Prediction of All Clinical and VWMS Values by ASCs (Independents)

Dependent Variable	Category	View	R ² (No. ASCs)	
Biplane ED volume	Volumes	4C + 2C	0.949 (19)	
Biplane ES volume		4C + 2C	0.936 (16)	
Biplane ejection fraction		4C + 2C	0.952 (28)	
ED sphericity		4C + 2C	0.893 (19)	
ES sphericity		4C + 2C	0.930 (17)	
Total (all 13 segments)	VWMS multiple segments	All	0.838 (24)	
Total 4C + 2C (9 segments)		4C + 2C	0.781 (15)	
Total 4C (5 segments)		4C	0.786 (19)	
Total 2C (5 segments)		2C	0.798 (21)	
Septal (2 segments)		4C	0.511 (14)	
Lateral (2 segments)		4C	0.668 (22)	
Anterior (2 segments)		2C	0.660 (18)	
Inferior (2 segments)		2C	0.701 (15)	
Apex		VWMS single segments	4C + 2C	0.753 (13)
Septal basal			4C	0.409 (9)
Septal mid	4C		0.668 (15)	
Lateral basal	4C		0.466 (13)	
Lateral mid	4C		0.675 (24)	
Anterior basal	2C		0.376 (16)	
Anterior mid	2C		0.643 (15)	
Inferior basal	2C		0.744 (20)	
Inferior mid	2C	0.614 (16)		
Single segment averages ± standard deviation			0.595 ± 0.142 (15.7 ± 4.3)	

VWMS, visual wall motion scoring; ED, end-diastole; ES, end-systole; ASC, AAM shape coefficients; 4C, four chambers; 2C, two chambers.

127 variables resulted in undesired statistical effects such as “over-training” (see the following section). Therefore only the major 25 ASCs of both views were used, giving a total of 52 variables. These 25 major eigenvectors were responsible for about 95% of total shape variabilities.

The regressions were performed for an optimized subset of ASCs. All ASCs with a low correlation to VWMS were eliminated to get an optimal prediction of VWMS from a minimal number of ASCs (using the “backward” method of independent variable selection in linear regression in SPSS). The resulting R² value and the remaining number of ASCs are reported.

Global volume measures (biplane ED, ES volumes, EF, and ED and ES sphericity) are very well predicted by shape (ASCs), which is not surprising because these measures are calculated directly from the ED and ES contours, which form a subset of the contours defining the ASCs.

A clear relation was found between ASCs and the different VWMS measures, although sometimes a large number of ASCs (9–24) was needed to get an optimal regression. In the prediction for single segments, most of

the basal segments (anterior basal, septal basal, and lateral basal) performed relatively poorly. The apex performed relatively well, maybe because the combined four-chamber and two-chamber parameters were used together. From the two-segment combinations, inferior performed relatively well, probably because of the good performance of the inferior basal segment. These differences between segments may be caused by the distributions of WMA over the segments, the visibility of different segments, or particularities in the VWMS scoring or border tracing. In general, results were relatively better when more segments were combined, which is partly an effect of averaging, partly of the longer total range of results (Fig. 3). Regression plots for the prediction of the total VWMS and for a single segment (apex) are given in Fig. 3.

Linear Discriminant Analysis

Discriminant analysis was performed to find optimal classification of WMA from a minimal number of ASCs. Because VWMS is a visually established, subjective assessment with considerable observer variability, wall motion score values were grouped into only two classes for

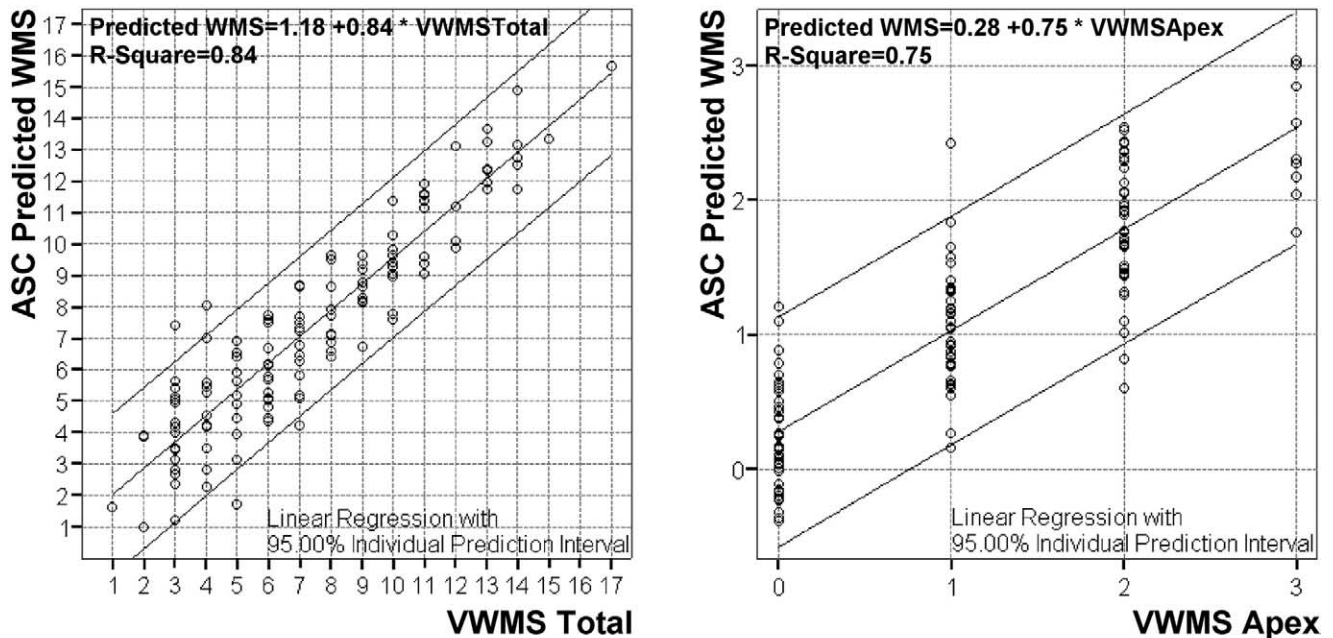


Figure 3. Multivariate linear regression: visual wall motion scoring total (sum of all 13 segments) versus prediction from 24 active appearance motion models (AAMM) shape coefficients (ASCs) of four-chamber and two-chamber active appearance motion models and visual wall motion scoring of apex (single segment) predicted from 13 ASCs.

these classification experiments. For single segments and combinations of 2 segments, a distinction was made between normal and abnormal wall motion, in which a score of 0 was considered normal, and all scores >0 abnormal. For combinations of 5 and more segments, in which many scores are summed, such a distinction would result in very biased or even empty classes (note that the patient set contained only infarct patients and no normals). Therefore, for these multisegment combinations a distinction into mild and severe WMA was made. For groups of 5 segments, a summed score >1 was considered severe; for the 9-segment combination, of four-chamber and two-chamber segments, >3 ; and for the total score of 13 segments, >5 . This corresponds to an average segmental score threshold of 0.4 and resulted in reasonably balanced groups in most cases.

Classification was performed in two different experiments, representing an ideal situation, and a worst-case situation. As described previously, the patient set was split in a TRN set ($n = 65$) and a TST set ($n = 64$). The shape model was trained from the TRN set only and thus is capable of modeling the TRN shapes almost exactly; therefore, the ASCs describe these shapes very accurately. For the TST set, the shapes were projected onto the shape model and approximated. However, these ASCs may not perfectly describe the shapes, because the training was

performed on a limited set only and may not completely cover all variability in the TST set. The ASCs derived for the TST set may also have slightly different characteristics with respect to WMA than those from the TRN set.

To assess the differences between these situations, two experiments were performed. First of all, the classification was performed on the TRN set, representing ASCs from a "perfect" shape model (corresponding to a shape model trained from a very large and well-balanced patient set). The classifier was trained using a leave-one-out approach: in turn, each of the training cases was left out, the optimal discriminant function was determined from the other cases, and tested on the one remaining case. This was repeated $n - 1$ times. This approach guarantees independence between training and test cases.

Secondly, a classifier was trained on ASCs from all TRN cases and tested on those of all TST cases. This is a worst-case, real-world experiment: both shape model and classifier are trained from a limited training set and tested on completely new shapes.

Linear discriminant analysis results on the prediction of VWMS are listed in Table 2. For comparison, the ASC predictions were set against the best predictor from the volumetric parameters: biplane EF. Note that this parameter should *not* be considered a gold standard for segmental VWMS prediction because it is associated only with

Table 2
Classification Correctness of Wall Motion Abnormality for Different Segments and Combinations

Classification Correctness (%)			Predicted From AAM Shape Coefficients (No. ASCs Employed)		Predicted From Biplane Ejection Fraction		
VWMS (Criterion)	Category	Views (No. Segments)	TRN	TST	TRN	TST	
Total (>5)	VWMS multiple segments	All (13)	100% (35)	77% (35)	85%	73%	
Total 4+2 (>3)		4C/2C (9)	89% (11)	70% (11)	75%	83%	
Total 4c (>1)		4C (5)	88% (13)	78% (13)	79%	77%	
Total 2c (>1)		2C (5)	100% (21)	97% (21)	65%	64%	
Septal (>0)		4C (2)	100% (28)	67% (28)	66%	72%	
Lateral (>0)		4C (2)	82% (10)	70% (10)	69%	73%	
Anterior (>0)		2C (2)	94% (11)	73% (11)	68%	69%	
Inferior (>0)		2C (2)	94% (16)	75% (16)	54%	45%	
Apex		VWMS single segments (criterion: >0)	4C/2C	94% (7)	81% (7)	75%	72%
Septal basal			4C	87% (10)	70% (10)	74%	58%
Septal mid	4C		92% (12)	73% (12)	63%	70%	
Lateral basal	4C		86% (8)	64% (8)	71%	63%	
Lateral mid	4C		77% (6)	70% (6)	69%	75%	
Anterior basal	2C		95% (3)	95% (3)	86%	86%	
Anterior mid	2C		94% (11)	75% (11)	68%	70%	
Inferior basal	2C		85% (5)	72% (5)	55%	58%	
Inferior mid	2C		91% (12)	66% (12)	63%	50%	
Single segment averages \pm standard deviation			88.9 \pm 5.9% (8.2 \pm 3.2)	74.0 \pm 9.4% (8.2 \pm 3.2)	69.4 \pm 8.8%	66.7 \pm 10.8%	

AAM, active appearance model; VWMS, visual wall motion scoring; TRN, training set; TST, testing set; 4C, four chambers; 2C, two chambers.

global LV function. Two different experiments were performed as described above.

Table 2 shows good ASC classification of WMA (64%–95% correctness for TST set) for both single (on average, 74%) and combined (multiple) segments. The numbers of ASCs employed were generally low (on average, 8 for single segments) except for a few combined cases in which the discriminant seemed to overtrain itself to cover 100% of the variation in the training data. In such cases, it would be possible to limit the number of included ASCs (probably at the cost of a lower performance). In the worst-case experiment, still a 74% correctness for single segments was achieved, which certainly is a promising result considering the variabilities in VWMS. The TRN test suggests that with an optimal shape model, a segmental correctness of up to 89% is feasible.

ASCs predict WMA better than EF in most cases, both for combined segments and single segments. As

expected, the difference is largest for single segments, in which EF predicts not much better than a random choice (50%). It could be seen as a biased guess: a reduced EF can tell that there must be a wall motion abnormality somewhere for a specific case, but it cannot tell you where. For the TRN set, ASC performs better in all cases; for the TST set, EF is sometimes slightly better, but this is probably an accidental effect. For both sets, the ASC single-segment average was significantly higher than the corresponding EF average, according to a single-sided paired *t*-test at the 1% level.

Two-chamber results were generally superior to four-chamber; this may be attributed to the distribution of WMA over the segments, where the two-chamber segments saw a wider range of VWMS scores.

Note that the prediction of total VWMS for all 13 segments is at least as good as that of the nine segments (four- and two-chamber only). This may sound strange,

because the extra segments (belonging to the long axis view) are not included in the ASCs at all. However, this may be attributed to the high correlation between the long-axis segments and their neighbors in the four- and two-chamber views, which are supplied by the same coronary arteries.

DISCUSSION

As the most important result from this study, we can conclude that ASCs are indeed suitable for classification of wall motion abnormalities. It also shows that endocardial contours (by themselves) may be sufficient to allow automated classification/prediction of VWMS, and that our proposed approach of endocardial border detection and subsequent shape analysis is feasible in principle.

Another interesting result is that an ASC shape analysis can assess the quality of sets of contours through direct correlation with clinical parameters. The percentage of variability of the clinical parameter explained by a linear combination of ASCs (R^2) is a useful measure for this. This also allows comparisons between different sets of contours (eg, manual versus automatically detected). Apart from these interesting first results, several issues remain to be treated.

Manually Versus Automatically Detected Contours

It remains to be shown that the described approach will also work on automatically determined contours (preferably determined by an AAM). All above experiments were performed on an 'expert-verified' contour set. This set was >80% derived semiautomatically, but the most important contours (ED and ES) were defined manually by the expert and subsequently detected contours were corrected; therefore, we consider it closer to a manually defined set. We only performed some preliminary experiments on contours that were detected fully automatically by AAMM, but results were less good than for the original set. Most likely, small errors in the detection tend to obscure the typical patterns seen in the manual contours. As we have seen with earlier studies (13,15,19), it seems that AAMs tend to stay a bit too close to the average shape/motion patterns. They generate quite a good overall approximation of the shapes (in terms of distances and area differences), but fail to follow the finer details. Luckily, as we have described earlier (19), there are still many possibilities to optimize the border detection, which is a subject for further studies.

Limitations of VWMS

It should be stressed that the strength of the found relations must be seen in the light of the large inherent uncertainties and variabilities associated with VWMS itself. The fact that on average 60% of the total variability in single-segment VWMS can be explained from a limited number (approximately 16) of ASCs is actually a strong result.

VWMS is in fact a qualitative measure made semi-quantitative, which makes it less suitable for a linear regression approach as applied here. Single segments can only have a few different scores and because of the small numbers of examples the distributions are quite irregular, so correlations and linear regression may be weak. Furthermore, VWMS is known to be subjective and operator-dependent. Even in highly controlled multicenter studies, it has been shown that interinstitution variability can be high. Although such numbers cannot be compared directly, eg 73% agreement on normality/abnormality of a complete dobutamine stress test was reported (2).

One should realize that automating or imitating VWMS is not the main goal. VWMS is a tool to predict the presence of coronary artery disease, and its virtues for that have been assessed well by comparison to established clinical measures, such as quantitative coronary angiography. It has also been compared with competing techniques such as the nuclear imaging thallium stress test and electrocardiogram stress testing. Therefore, it would be most interesting to relate ASC shape analysis directly to quantitative coronary angiography to determine its sensitivity and specificity for detection of coronary artery disease. It could also be related to other established measures of coronary or myocardial pathology.

Relations With Volumetric Parameters

From the volumetric parameters, it was found that only EF correlated well to global VWMS. Sphericity indices showed poor relations, and biplane volumes offered no additional value. Predictive power for segmental VWMS was very low, as can be expected.

However, these weak relations stress the fact that VWMS and ASCs are indeed closely related, and that both global and segmental VWMS can be predicted from ASCs. The weak relations also rule out the possibility that by using a large number of ASC variables we could predict almost anything; this obviously is not the case. The found relations are real and not statistical artifacts. Furthermore, the fact that ASCs can predict any of the

volumetric parameters is another proof that they cover the properties of shape well.

Alternatives for Assessment of Wall Motion Abnormalities

In this study, we have chosen to analyze endocardial borders to detect wall motion abnormalities. As mentioned, alternative approaches exist, such as tissue Doppler imaging or the derived strain rate (20) and strain imaging (21). Without going into details, we can state that these techniques are limited as well. In particular, we have shown that combining longitudinal velocities from tissue Doppler imaging with radial velocities from endocardial border detection may increase success (6).

Another possibility is the addition of epicardial contours. In VWMS, thickening of the myocardium is an important clue for normal contraction. Assessment of myocardial thickness/thickening would involve both endocardium and epicardium. However, the epicardium is often hard to delineate precisely from echocardiographic data. Although an AAM approach allows for multiple contours to be modeled and detected simultaneously, it remains to be studied whether this will improve WMA classification.

PCA Limitations, Extensions, and Alternatives

The described PCA-based approach has some limitations. As with any training-based approach, its reliability depends on the range of variabilities covered in the training set: it should include normals and sufficient cases of expected pathologies. Furthermore, the result is limited by the quality and reproducibility of the training contour data: accurately validated borders on substantially larger data sets are required.

In this study, almost all shape variation (99.9%) from the training set was included in the models and analyses, except for the combined views where 95% was used. Removing a larger percentage of variation would result in a more generalized and compact model. However, we should probably use larger training sets to achieve good generalization.

PCA will provide an optimal description of variability over a set, but is not aimed at an optimal classification or localization. This is a reason why relatively many ASCs are involved in single segment and multisegment VWMS prediction or WMA classification. For this purpose, techniques such as independent component analysis may form a good alternative for PCA, allowing us to decompose

shapes into components that describe very local shape behavior. This is a subject of further study.

PCA shape modeling is an inherent part of AAM methods, and it is therefore attractive to combine AAM border detection with ASC shape analysis. However, the ASC analysis can be applied completely independent of AAMs and can be combined with any type of border detection.

Limitations of the Study Setup

The setup of this study was limited in several aspects. Only infarct patients were included, whereas for a good unbiased general shape model training and ASC discriminant function determination, other pathologies, and normals should be included as well. From the stress echoes, only resting two- and four-chamber images were used. Adding long-axis and short-axis images may improve results. The same approach should be tested on the dobutamine images, and on the assessment of rest/stress differences. A combined shape model for rest and stress images could be trained as well.

For the statistical analyses, only linear regression and linear discriminant classifiers were employed, whereas VWMS is a nonlinear measure. Other nonlinear classifiers may achieve better results.

CONCLUSIONS

AAM shape coefficients can describe regional wall motion abnormality and can be used for automated classification of such abnormalities with good accuracy: for single segments, on average 89% correctness was achieved against an expert observer in case of a "perfect" shape model. With a worst-case shape model, 74% correctness was obtained. Considering the inaccuracy and high interobserver and intraobserver variability of visual scoring, the achieved results suggest that automated wall motion scoring is feasible.

VWMS and endocardial border shape/motion patterns are shown to be closely related; if accurate automated border detection is available, this opens the way to fully automated classification of wall motion abnormality in echocardiograms.

ASC shape analysis is also a powerful tool for evaluating the relation of shapes with arbitrary clinical parameters or for comparing the quality of different contour sets by direct comparison with clinical measures.

ACKNOWLEDGMENT

Data analysis support provided by Gerard van Burken is gratefully acknowledged.

REFERENCES

1. Marwick TH. Stress echocardiography: its role in the diagnosis and evaluation of coronary artery disease. 2nd ed. Dordrecht, The Netherlands: Kluwer, 2003.
2. Hoffman R, Lethen H, Marwick TH, et al. Analysis of interinstitutional observer agreement in interpretation of dobutamine stress echocardiograms. *J Am Coll Cardiol* 1996; 27:330-336.
3. Assman PA, Slager CJ, van der Borden SG, Tijssen JG, Oomen JA, Roelandt JR. Comparison of models for quantitative left ventricular wall motion analysis from two-dimensional echocardiograms during acute myocardial infarction. *Am J Cardiol* 1993; 71:1262-1269.
4. Fry SJ, Hunziker P, Bosch H, et al. Automated echocardiographic confirmation of regional wall motion abnormalities: quantitation of continuous LV volume [Abstract]. *J Am Coll Cardiol* 1998; 31(Suppl A):56A.
5. Hunziker P, Yuan D, Schöb L, et al. Objective and quantitative stress echo analysis to diagnose coronary disease using model-based image processing [Abstract]. *J Am Coll Cardiol* 2000; 35(Suppl A):431A.
6. Cain P, Short L, Baglin T, et al. Development of a fully quantitative approach to the interpretation of stress echo-cardiography using radial and longitudinal myocardial velocities. *J Am Soc Echocardiogr* 2002; 15:759-767.
7. Bosch JG, Savalle LH, van Burken G, et al. Evaluation of a semiautomatic contour detection approach in sequences of short-axis two-dimensional echocardiographic images. *J Am Soc Echocardiogr* 1995; 8:810-821.
8. Bosch JG, van Burken G, et al. Overview of automated quantitation techniques in 2D echocardiography. In: Reiber J, Wall EVD, eds. *What's new in cardiovascular imaging*. Dordrecht, Germany: Kluwer, 1998; 363-376.
9. Cootes TF, Edwards GJ, Taylor CJ. Active appearance models. In: Burkhardt H, Neumann B, eds. *European Conference Computer Vision*. Berlin: Springer, 1998; 484-498.
10. Cootes TF, Taylor CJ. Statistical models of appearance for medical image analysis and computer vision. In: Sonka M, Hanson KM, eds. *Medical imaging 2001: image processing*, Proc SPIE 2001; 4322:236-248.
11. Cootes TF, Hill A, Taylor CJ, et al. Use of active shape models for locating structures in medical images. *Image Vision Comp* 1994; 12:355-366.
12. Bosch HG, Mitchell SC, Lelieveldt BPF, et al. Active appearance motion models for endocardial contour detection in time sequences of echocardiograms. In: Sonka M, Hanson KM, eds. *Medical imaging 2001: image processing*. Proc SPIE 2001; 4322:257-268.
13. Bosch JG, Mitchell SC, Lelieveldt BPF, et al. Automatic segmentation of echocardiographic sequences by active appearance motion models. *IEEE Trans Med Imaging* 2002; 21:1374-1383.
14. Bosch JG, Mitchell SC, Lelieveldt BPF, et al. Fully automated endocardial contour detection in time sequences of echocardiograms by three-dimensional active appearance models. In: Sonka M, Fitzpatrick JM, eds. *Medical imaging 2002: image processing*. Proc SPIE 2002; 4684:452-462.
15. Mitchell SC, Bosch JG, Lelieveldt BPF, et al. 3-D active appearance models: segmentation of cardiac MR and ultrasound images. *IEEE Trans Med Imaging* 2002; 21:1167-1178.
16. Bosch JG, Nijland F, Mitchell SC, et al. Automated classification of wall motion abnormalities by principal component analysis of endocardial shape motion patterns in echocardiograms. In: Sonka M, Fitzpatrick JM, eds. *Medical imaging 2003: image processing*. Proc SPIE 2003; 5032:38-49.
17. Sonka M, Bosch JG, Lelieveldt BPF, et al. Computer-aided diagnosis via model-based shape analysis: cardiac MR and echo. In: Lemke HU, Vannier MW, Inamura K, et al., eds. *Computer aided radiology and surgery*. Elsevier, 2003; 1013-1018.
18. Nijland F, Kamp O, Verhorst PMJ, et al. Myocardial viability: impact on left ventricular dilatation after acute myocardial infarction. *Heart* 2002; 87:17-22.
19. Mitchell SC, Lelieveldt BPF, van der Geest RJ, Bosch HG, Reiber JHC, Sonka M. Multistage hybrid active appearance model matching: segmentation of left and right ventricles in cardiac MR images. *IEEE Trans Med Imaging* 2001; 20:415-423.
20. Heimdal A, Stoylen A, Torp H, et al. Real-time strain rate imaging of the left ventricle by ultrasound. *J Am Soc Echocardiogr* 1998; 11:1013-1019.
21. Armstrong G, Pasquet A, Fukamachi K, et al. Use of peak systolic strain as an index of regional left ventricular function: comparison with tissue Doppler velocity during dobutamine stress and myocardial ischemia. *J Am Soc Echocardiogr* 2000; 13:731-737.